UNIVERSITY OF CALIFORNIA
RIVERSIDE

Altered Water Diffusivity in Mouse AQP4$^{-/-}$ Brain During Development Using Diffusion Tensor Imaging

A Thesis submitted in partial satisfaction
of the requirements for the degree of

Master of Science

in

Neuroscience

by

Gi Eun Yang

June 2012

Thesis Committee:
Dr. Devin Binder, Chairperson
Dr. Todd Fiacco
Dr. Andre Obenaus

ProQuest LLC.
789 East Eisenhower Parkway
P.O. Box 1346
Ann Arbor, MI 48106 - 1346

The Thesis of Gi Eun Yang is approved:

_____

_____

_____
Committee Chairperson

University of California, Riverside

ACKNOWLEDGEMENTS

I would like to express my sincere thanks and appreciation to my thesis chair and academic advisor, Dr. Devin Binder. Without his valuable advice, patience, never-ending support and encouraging words, this thesis would not have been possible. He believed in me when I didn't believe in myself and he fought for me when I needed it most. Never before has anyone worked so hard to keep me around and believed so much in me. It's truly been an honor working in his laboratory.

I would also like to thank my other thesis committee members, Dr. Todd Fiacco and Dr. Andre Obenaus, for their support and expertise. Their assistance with experiments, collaborative work, and use of equipment is much appreciated but pales in comparison to the value of their support.

I would like to give special thanks to the members of the Binder & Obenaus Lab who assisted me both mentally and physically with my experiments: Mike Hsu, Sonny Kim, Kamal Amamdipudi, Lei Huang, Shu-Wei Sun, Arash Adami, Virginia Donovan and Alena Yusof.

Additionally, I would like to thank my friends and loved ones outside the Binder Lab who supported me every step of the way: Becca Post, Jean Shin, Won Ha and Mr. G.

ABSTRACT OF THE THESIS

Altered Water Diffusivity in Mouse AQP4$^{-/-}$ Brain During Development Using Diffusion Tensor Imaging

by

Gi Eun Yang

Master of Science, Graduate Program in Neuroscience
University of California, Riverside, June 2012
Dr. Devin Binder, Chairperson

Aquaporin-4 (AQP4) is the glial water channel that is primarily expressed in astrocytes. Various roles of AQP4 have been previously discussed such as deletion of AQP4 induces enlarged extracellular space. However, the role of AQP4 in brain water diffusivity is not well described. In this study, we investigated the developmental changes of brain water diffusivity in relation to development and presence of AQP4 channels in AQP4$^{+/+}$ and AQP4$^{-/-}$ animals using diffusion tensor imaging (DTI) and brain water content analyses. DTI results revealed a developmental decrease in water diffusivity in both AQP4$^{+/+}$ and AQP4$^{-/-}$ genotypes. AQP4$^{-/-}$ mice exhibited an increased diffusivities as juveniles but later deceased in adulthood. Brain water content analysis revealed greater water content in AQP4$^{-/-}$ mice, which suggests the effect of enlarged extracellular space resulting in greater basal water content. The results highlight the role of AQP4 channels in the regulation and mediation of brain water mobility.

TABLE OF CONTENTS

Page

LIST OF FIGURES

Introduction

Aquaporins (AQPs) are small integral membrane proteins that locate in the membrane of biological cells (Verkman 2002; Agre 2006). AQPs assemble as tetramers, and six membrane spanning domains (~30 kDa monomer) surround a water pore that allows bidirectional water flow (Verkman 2005). Aquaporins selectively direct water molecules in and out of the cell, and blocks ions and other solutes to pass through. Multiple AQPs are known to exist in mammals and plants. In mammals, they are expressed in endothelial, epithelial and other tissues (Verkman 2005). The AQPs: AQP0, AQP1, AQP2, AQP4, and AQP5 only transport water, while AQP3, AQP7 and AQP9 transport water and glycerol (aquaglyceroporins) (Agre *et al*. 2002; Verkman 2002).

Aquaporin 4 (Figure 1) is believed to play a key role in regulating water and ion homeostasis in the central nervous system (CNS) by allowing bidirectional water flow across plasma membranes (Verkman *et al*. 2006). A seven-fold decrease in water permeability in $AQP4^{-/-}$ astrocytes were observed compared to $AQP4^{+/+}$ as evidence (Solenov *et al*. 2004). AQP4 are mainly expressed in the brain and spinal cord, and are found in high concentrations at specialized membrane domains including astroglial endfeet in contact with blood vessels and astrocyte membranes that ensheathe synapses (Nielsen *et al.* 1997; Nagelhus *et al*. 2004). Other sites include glia limitans and subependymal astrocytes (Nielsen *et al*. 1997). Several studies have shown that AQP4 is important in brain water transport and clearance of brain water in both normal

and pathological conditions (Manley *et al*. 2004; Papadopoulos *et al*. 2004; Badaut *et al.* 2011).

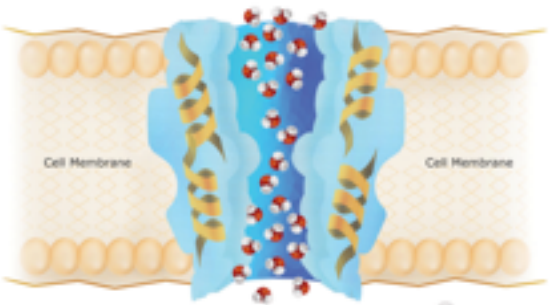

Figure 1. A schematic diagram of AQP4 channel. AQP4 is expressed by glial cells and located highly at membrane domains: (1) astroglial endfeet in contact with blood vessels and (2) synapse ensheathing astrocyte membranes. It allows bidirectional water flow across plasma membranes.

AQP4$^{-/-}$ mice do not display gross morphological, neurological abnormality or impaired osmoregulation compared to AQP4$^{+/+}$ types (Hsu *et al*. 2007). The deletion of AQP4 channels shows no effect in baseline CNS characteristics, such as anatomy of cerebral vessels, intracranial pressure or lateral ventricle volume (Manley *et al*. 2000; Papadopoulos and Verkman 2005; Bloch *et al*. 2006). According to Saadoun and colleagues, AQP4$^{-/-}$ mice showed no differences in neurons, astrocytes and oligodendrocytes characteristics to that of AQP4$^{+/+}$ mice (Saadoun *et al*. 2008). However, detailed studies have demonstrated reduced osmotic water permeability in *in vivo* and *ex vivo* AQP4$^{-/-}$ mice brain (Thiagarajah *et al*. 2005). The differences they manifest are mild impairments in maximal urine-concentrating ability and expansion of extracellular space (Ma *et al*. 1997; Yao *et al*. 2008). Although the general differences seem minimal, the effect of AQP4 channels on brain edema and seizure are potentially immense.

The deletion of AQP4 enhances the outcome of cytotoxic edema by reducing cell swelling in models of water intoxication and cerebral ischemia (Manley *et al*. 2000). The development of hemispheric brain swelling 24h after middle cerebral artery occlusion (MCAO) experiments showed 35% less swelling in AQP4$^{-/-}$ mice compared to AQP4$^{+/+}$ mice (Manley *et al*. 2000). On the contrary, the deletion of AQP4 has a detrimental outcome in cases of vasogenic edema caused by brain tumors (Papadopoulos *et al*. 2004), brain abscess (Bloch *et al*. 2005) and kaolin-induced obstructive hydrocephalus (Bloch *et al*. 2006).

Previous studies also point a major role of AQP4 in neuronal excitability. Studies conducted by Binder *et al.* found that AQP4$^{-/-}$ mice have remarkably prolonged seizure duration and impaired K+ reuptake in AQP4$^{-/-}$ mice in response to direct cortical stimulation (Binder *et al*. 2004; Binder *et al*. 2006). Human data from hippocampal sclerosis specimens suggested alterations in AQP4 expression leading to impairment of AQP4 function (Lee *et al*. 2004). However, the mechanism by which AQP4 expression is altered during the development of epilepsy still needs to be elucidated. Lee and colleagues have examined the role of AQP4 in an epileptic model of spontaneous recurring seizures to determine the impact of water homeostasis in the epileptogenic period. They discovered that both AQP4$^{+/+}$ and AQP4$^{-/-}$ mice developed status epilepticus (SE, a state of persistent seizure) after initial seizure induction, a significant reduction of AQP4 expression in hippocampus on post SE day 1 which slowly increased with time, and increased tissue water content inversely related to AQP4 expression (Lee *et al*. 2012).

AQP4 is also a key component of astrocyte migration (Tait *et al*. 2008). Reduction in the migration of AQP4$^{-/-}$ astrocytes to a wound site has been reported (Auguste *et al*. 2007). In addition, delayed glial scarring after a cortical stab injury in AQP4$^{-/-}$ mice has been reported (Saadoun *et al*. 2005).

Extracellular space (ECS) mostly occupied by the extracellular matrix (ECM) and by the interstitial fluid (ISF), has been discussed to be greater in AQP4$^{-/-}$ in multiple studies. To assess diffusion properties of ECS, extracellular

volume fraction (α) and tissue tortuosity (λ) is used. Extracellular volume fraction is determined by acquiring the ratio of ECS volume to whole tissue volume, and tissue tortuosity is inferred by measuring path length for diffusion between two points that are formed due to cellular membranes forming barriers (Nicholson and Philips 1981). Surface photobleaching (FRAP), fiberoptic photobleaching and tetramethylammonium (TMA+) experiments suggested enlarged ECS in AQP4$^{-/-}$ mice (Binder *et al*. 2004; Yao *et al*. 2008; Zador *et al*. 2008). Based on *in vivo* and *in vitro* work of Yao and colleagues, it was suggested that AQP4$^{-/-}$ mice have 28% larger extracellular volume fraction with no difference in tissue tortuosity (Yao *et al*. 2008). Due to this factor, AQP4$^{-/-}$ mice are claimed to have an increased seizure threshold as well as extended seizure duration (Binder *et al*. 2004; Binder *et al*. 2006).

Diffusion tensor imaging (DTI) is an MRI technique that detects the directionality of white matter (WM) fibers within the CNS and characterizes white matter tracts (Mori *et al*. 2001; Sun *et al*. 2003). Water diffusion detected by diffusion tensor imaging (DTI) measure extracellular, intracellular, and transcellular diffusivity. Changes in these diffusivities often indicate changes in brain biology, such as demyelination of axons or ischemic injury (Obenaus and Ashwal 2008). Also, the disruption of WM structural integrity can be assessed in cases of diffuse axonal injury caused by TBI (Cubon *et al*. 2011; Blumbergs *et al*. 1994).

Eigenvalues ($\lambda_{\parallel}$ and $\lambda_{\perp}$), or diffusivities (Figure 2), are used to diagnose various conditions including axonal and myelin injury (Sun *et al*. 2003). Axial diffusivity, λ_1 or $\lambda_{\parallel}$, describes the water movement parallel to the axonal fibers and is thought to report the degree of axonal integrity. When axonal injury occurs, axial diffusivity is expected to initially decrease due to reseal of severed axons, as well as retraction of large axons that compress ECS around axons (Brody *et al.* 2007). Radial diffusivity, λ_2 and λ_3, or $\lambda_{\perp}$, measures water diffusion perpendicular to the axonal fibers, and is used to determine myelin integrity. Radial diffusivity may increase when to demyelination occurs which increases the ECS between axons (Alexander *et al.* 2007). Relative anisotropy (RA; 1/fractional anisotropy (FA)), a variance of all diffusivity directions, measures the directional asymmetry of diffusion (Arfanakis *et al.* 2002; Wilde *et al.* 2008). Reduced RA values are expected to be seen in cases of traumatic axonal injury, which decreases **axial** diffusivity (Brody *et al.* 2007). Lastly, trace diffusivity is the sum of axial and radial diffusivities. Damage to myelination may increase trace diffusivity, whereas axonal injury may decrease trace diffusivity (Gönenç *et al.* 2010).

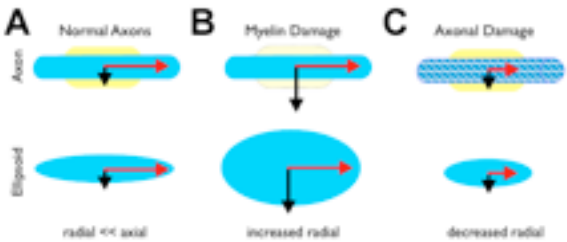

Figure 2. A schematic diagram of diffusion tensor imaging (DTI) measurements. (A) In normal conditions, intact white matter (WM) tracts (blue = axons, yellow = myelin sheath) allow water to diffuse along the axon (red arrow; axial diffusivity) dominantly compared to perpendicular to the axon (black arrow; radial diffusivity). This also can be represented as diffusion ellipsoid (blue ellipsoid). (B) When myelin damage occurs, water can freely diffuse perpendicularly to the axon, thus increases radial diffusivity. Ellipsoid diagram represents increased radial diffusivity. (C) With axonal damage, water movement parallel to the axon is hindered. However, due to intact myelin sheath, radial diffusivity does not change. Ellipsoid diagram represents decreased axial diffusivity. Adopted from Obenaus and Jacobs 2007.

Previous reports have demonstrated excellent concordance between *ex vivo* brains and *in vivo* samples. Previously, Sun *et al* have found that axial diffusivity, radial diffusivity and RA values do not differ from *in vivo* to *ex vivo* scans. One key advantage of using *ex vivo* brains is the use of longer imaging time to allow for detailed data acquisition and analysis. Motion artifacts are an issue during *in vivo* scans, as well as the required shorter imaging time when using living subjects under anesthesia, thus *ex vivo* imaging improves on signal to noise (SNR) (Sun *et al*. 2003).

The role of AQP4 in brain water diffusivity has not been studied in the context of DTI. Recently, a study on silencing AQP4 channels *in vivo* using small interfering RNA (siRNA) observed decreased apparent diffusion coefficient (ADC) values, an average of all eigenvalues (Badaut *et al*. 2011). Badaut and colleagues suggested that this may be a result of *in vivo* astrocytic AQP4 inhibition (Badaut *et al*. 2011). Collectively, these findings propose a significant involvement of astrocytic AQP4 channels on water diffusion and different ECS property due to the deletion of AQP4 in brain tissues.

Although previous studies have observed histological outcomes in AQP4$^{-/-}$ mice, no study has analyzed changes in water diffusion using non-invasive methods. Therefore, we hypothesized that astrocytic AQP4 channels and the characteristic of enlarged ECS in AQP4$^{-/-}$ mice significantly alter brain water diffusivity, and diffusivity modifies with brain development (Figure 3). Using DTI analysis of WM (corpus callosum) and gray matter (GM; cortex), with wet/dry

mass method and immunohistochemistry (IHC) will result in discovering correlation between brain water diffusivity and AQP4 expression.

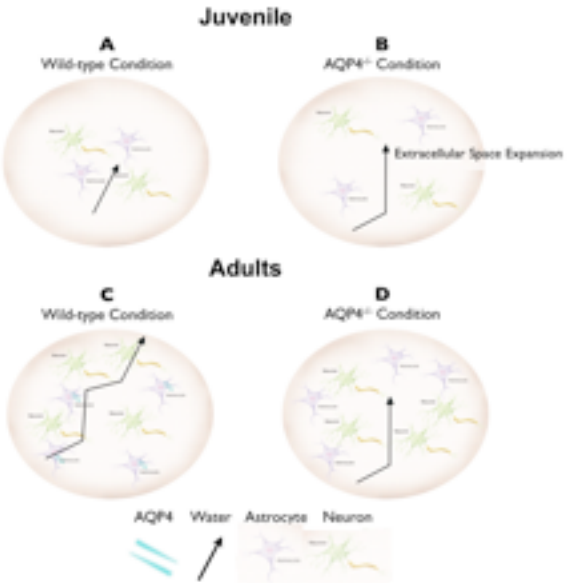

Figure 3. Hypothesis of water diffusion differences in juvenile and adult brain tissue. We hypothesize that water diffusion is decreased in juvenile AQP4$^{+/+}$ brains (A) in comparison to juvenile AQP4$^{-/-}$ brains (B) due to enlarged extracellular space (ECS) in AQP4$^{-/-}$ tissue facilitating higher water mobility. In adult AQP4$^{+/+}$ animals (C), water diffusion is higher compared to adult AQP4$^{-/-}$ animals (D) due to the presence of AQP4 channels facilitating accelerated water movement. In adults, we hypothesize that the effect of AQP4 channel deletion overrides enlarged ECS factor in diffusivity. Adopted from Badaut *et al*. 2011.

Materials and Methods

Subjects

All experiments were conducted under the guidelines set by the National Institutes of Health and were approved by the University of California, Riverside Institutional Animal Care and Use Committee (IACUC).

Male AQP4$^{-/-}$ mice with CD1 genetic background were generated by targeted gene disruption at the University of California at San Francisco (Ma *et al*. 1997). CD1 genetic background male AQP4$^{+/+}$ and AQP4$^{-/-}$ mice were used in the present study. Animals were house under 12 hour light/12 hour dark controlled conditions. Food and water were provided to the mice *ad libitum.*

Number of Mice

Total of 54 mice were used. Brains for DTI analysis and IHC were obtained from postnatal days (P) 15, and P73 ± 5.75 and P94 ± 3 (n=9 for each genotype; Table 1). P16 ± 3, P82 ± 2 and P105- mice were used for brain water content analysis (n= 24, 6, 6 respectively).

Tissue Processing

For DTI and IHC analysis, animals were deeply anesthetized with ketamine/xylazine mixture. Subjects were then transcardially perfused with 4% paraformaldehyde (PFA). Skin removal was made from intact skull. Then brains with intact skull were transferred to vials containing PFA for overnight. Postfixed samples were then transferred into vials containing PBS until imaging.

Diffusion Tensor Imaging Experiments

Perfused and dissected AQP4$^{+/+}$ and AQP4$^{-/-}$ *ex vivo* brains (n=9 for each genotype) were placed in a RF solenoid coil (3 cm inner diameter) to act as the RF transmitter and receiver for the MR signal. Data were acquired in a Bruker Avance 11.7 T MRI (Bruker Biospin, Billerica, MA, USA). A 10 echo T2 and diffusion tensor sequences were acquired. Each sequence assessed 30 coronal slices, 0.5 mm slice thickness with a 1 mm interleave. The parameters of T2 sequences were: time to repetition (TR) = 1769.9ms, echo time (TE) = 10.2 ms, field of view (FOV) = 2 cm, matrix = 256 x 256, NEX (number of acquisitions) = 4 and acquisition time of 30 minutes. The spin echo diffusion sequences were: TR = 552.5 ms, TE = 15.1 ms, FOV = 2cm, matrix = 256 x 256, NEX = 4. Diffusion-sensitizing gradients (450 mT/m) were applied in six directions: [Gx, Gy, Gz] = [-0.7, 0, 0.7], [0, -0.7, 0.7], [-0.7, 0.7, 0], [0.7, 0, 0.7], [0, 0.7, 0.7] and [0.7, 0.7, 0]. *Ex vivo* DTI data set was obtained with an acquisition time of 8 hours.

Region of Interest (ROI) Data Analysis

Each diffusion-tensor image was derived to calculate for the six independent gradients of the diffusion tensor. The tensor maps were used to determine eigenvectors and eigenvalues (λ_1, λ_2, and λ_3) by matrix diagnolization (Sun *et al.* 2003). T2 and DTI maps were generated using custom software generated in Matlab (MathWorks, Natick, MA). Trace-normalized axial diffusivity (mm^2/sec), trace-normalized radial diffusivity (mm^2/sec), relative anisotropy and trace diffusivity (mm^2/sec) were calculated by the following equations:

$$\lambda_{\parallel} = \lambda_1 \quad [1]$$

$$\lambda_{\perp} = (\lambda_2 + \lambda_3) / 2 \quad [2]$$

$$\text{Trace diffusivity} = \lambda_1 + \lambda_2 + \lambda_3 \quad [3]$$

$$RA = \frac{\sqrt{(\lambda_1 - [D])^2 + (\lambda_2 - [D])^2 + (\lambda_3 - [D])^2}}{\sqrt{3}[D]} \quad [4]$$

where [D] is the mean of the diffusivity.

Region of interests (ROIs) were delineated on corpus callosum (CC; WM) and cortex (CTX; GM) above hippocampus of both T2 and DTI maps using Cheshire (Parexel International Corporation, Waltham, MA). 8-10 scan slices originating from anterior commisure and moving caudally were used for analysis for WM and GM visualization. Area of each ROI, mean, number of each pixels and standard deviation were extracted.

Histology Preparation

The fixed brains used for DTI analysis were put in 30% sucrose in PBS for 72 hours. Brains were then removed and frozen in isopentane (2-methyl butane) on dry ice. The frozen brains were kept in -80°C for storage and were cut in coronal sections with 50µm thickness at -16°C on a cryostat (Leica, Richmond, IL). Sectioned tissues were then transferred to 24-well plate filled with PBS.

Immunohistochemistry and Image Analysis

Floating sections were first blocked with 5% normal goat serum (NGS) / PBS for 1 hour in room temperature (RT). Incubation with primary antibodies rabbit anti-200 kD neurofilament (NF-200) (Sigma-Aldrich, St. Louis, MO; 1:1000)

Experiment	Number of P15 AQP4$^{+/+}$ mice used	Number of P15 AQP4$^{-/-}$ mice used	Number of P73 AQP4$^{+/+}$ mice used	Number of P73 AQP4$^{-/-}$ mice used	Number of P94 AQP4$^{+/+}$ mice used	Number of P94 AQP4$^{-/-}$ mice used	Total
DTI & IHC	3	3	3	3	3	3	18
Experiment	Number of P16 AQP4$^{+/+}$ mice used	Number of P16 AQP4$^{-/-}$ mice used	Number of P82 AQP4$^{+/+}$ mice used	Number of P82 AQP4$^{-/-}$ mice used	Number of P105 AQP4$^{+/+}$ mice used	Number of P105 AQP4$^{-/-}$ mice used	Total
Brain Water Content Analysis	12	12	3	3	3	3	36
							54

Table 1. Number of mice used for the study. Total of 18 mice were used for DTI and IHC analysis (n=9 each genotype). For brain water content analysis, total of 36 subjects were used (n=18 each genotype). All experiments were approved by the University of California, Riverside Institutional Animal Care and Use Committee (IACUC).

and rat anti-myelin basic protein (MBP) (Millipore, Temecula, CA; 1:1000) in PBS containing 0.1% Triton X-100 was performed, and stored in 4°C overnight with agitation. Anti NF-200 was used for assessing axonal integrity, and anti MBP was used for assessing myelin integrity. After PBS wash, secondary antibodies donkey-anti-rat IgG Alexa Fluor 594 (Invitrogen, Carlsbad, CA; 1:400) and goat-anti-rabbit IgG Alexa Fluor 488 (Invitrogen, Carlsbad, CA; 1:400) were added and incubated for 2 hours at room temperature (25°C). After mounting, sections were sealed with Vectashield (Vector Laboratories Inc., Burlingame, CA). Slides were then observed and processed using 20X fluorescent microscope (Zeiss Axioskop, Thornwood, NY).

Brain Water Content Measurement

Animals (P16, P82, P105) were anaesthetised via ketamine/xylazine injection (body weight (g) x 0.018) and decapitated (n=24). Then decapitated samples were dissected immediately. Cortical areas (excluding cerebellum and olfactory bulb) separated down the sagittal midline were weighed and placed in an oven (Fisher Scientific, Pittsburgh, PA) at 80°C for 48 h. After complete dehydration, brain samples were again weighed and % water content was calculated: [(wet mass - dry mass) / wet mass] x 100.

Statistical Analysis

Statistical analysis was performed using GraphPad Prism v4.0 (GraphPad Software, San Diego, CA). All data are presented as the means ± SEM. When comparing white and gray matter genotypes, we used unpaired *t*-tests. One-way

ANOVA was used for developmental comparison within genotype, and two-way ANOVA was used to compare differences between genotypes with time. *Post-hoc* (Bonferonni multiple comparison) analysis was performed when appropriate.

Results:

DTI was used to investigate the role of AQP4 channels on brain water diffusivity. Based on previous studies, it was hypothesized that juvenile $AQP4^{-/-}$ mice would have higher diffusivity compared to $AQP4^{+/+}$ animals due to enlarged ECS, and is reversed in adulthood due to the presence of AQP4 channels in $AQP4^{+/+}$ mice facilitating increased water mobility. Also, another sub-arching hypothesis was that diffusivity would modify with development due to the development of brain structures and astrocytes. Therefore, water diffusivity in $AQP4^{+/+}$ will increase above than $AQP4^{-/-}$ after brain development.

Genotype Analysis in $AQP4^{+/+}$ and $AQP4^{-/-}$

White Matter Genotype Analysis in $AQP4^{+/+}$ and $AQP4^{-/-}$

In order to evaluate water diffusivity in WM tracts in $AQP4^{-/-}$, we imaged intact mice skulls using T2 and DTI (Figure 4A and B). The axial diffusivity was significantly increased in $AQP4^{-/-}$ mice at P15 compared to $AQP4^{+/+}$, which may be a result of the enlarged ECS ($p<0.01$, Figure 5A). In contrast, these findings were reversed as the animals aged. The axial diffusivity in $AQP4^{-/-}$ mice were significantly lower than their $AQP4^{+/+}$ counterparts at P73 and P94 confirming the significant contribution of AQP4 channels facilitating water mobility in adulthood.

The radial diffusivity did not reveal any significant difference between genotype groups at P15 and P73 (Figure 5B). However, by P94, the radial diffusivity was significantly increased in $AQP4^{+/+}$ ($p<0.01$). This is indicative of

AQP4 channels in contact with myelin aiding water movement perpendicular to axonal direction.

Trace diffusivity was significantly increased in $AQP4^{-/-}$ mice at P15 compared to $AQP4^{+/+}$, indicating faster diffusion mediated by enlarged ECS ($p<0.05$, Figure 5C). However, at P73, the significance was not found. However, the trace diffusivity of $AQP4^{-/-}$ animals at P94 were found significantly lower than $AQP4^{+/+}$, confirming the activity of AQP4 allowing faster water diffusivity in $AQP4^{+/+}$ as adults ($p<0.05$).

There were no significant differences in RA throughout all age groups (Figure 5D). Our results confirm that there are no significant axonal and myelin differences between genotypes.

T2 values had contrasting results compared to DTI. At P15, we found a 35% decrease in T2 values in $AQP4^{-/-}$ compared to $AQP4^{+/+}$ ($p<0.001$, Figure 5E). At P73, statistical significance was not seen. However, the difference in T2 values at P15 returned at P93 where we observed a significant decrease in $AQP4^{-/-}$.

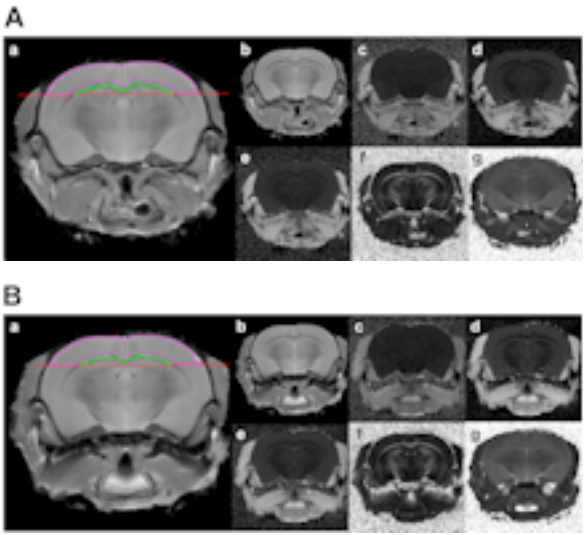

Figure 4. Representative DTI and T2 maps of *ex vivo* AQP4$^{+/+}$ and AQP4$^{-/-}$. (A) Regions of interests (ROI) (a) were drawn manually on a T2 image from an AQP4$^{+/+}$ mouse above hippocampus (red line) to analyze stereotactically identical areas. Corpus callosum (green outline) was drawn bilaterally to encompass the majority of the white matter fiber tracts. Cortex (magenta outline) was also drawn bilaterally to encompass the majority of the gray matter. (b) represents a raw T2 image before ROIs were drawn. These ROIs were transferred onto stereotactically matched maps those measure axial diffusivity (c), radial diffusivity (d), trace diffusivity (e), RA (f) and T2 signal (g). (B) Identical procedures were done on stereotactically matched AQP4$^{-/-}$ DTI maps (a-g, respectively). Note the similar anatomical morphology of the two genotypes.

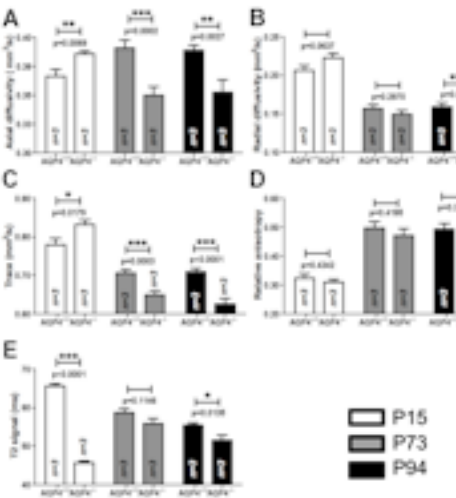

Figure 5. DTI and T2 analysis of white matter in AQP4$^{+/+}$ and AQP4$^{-/-}$ animals. (A) The axial diffusivity was significantly increased in AQP4$^{-/-}$ mice at P15 compared to AQP4$^{+/+}$. However, at P73 and P94, AQP4$^{+/+}$ demonstrated a higher diffusivity compared to AQP4$^{-/-}$. (B) Although we did not find any differences in the radial diffusivity between groups at P15 and P73, the radial diffusivity was significantly decreased in AQP4$^{-/-}$ at P93. (C) P15 trace diffusivity analysis revealed a significant increase in AQP4$^{-/-}$ at P15 followed by significant decrease in P73 and P94 of AQP4$^{-/-}$ mice. (D) RA analysis did not present statistical differences in all developmental stages. (E) T2 signal of AQP4$^{+/+}$ was significantly higher in P15 and P94. Statistical analysis was performed using unpaired *t*-tests (*p<0.05, **p<0.01, ***p<0.001). Abbreviations: P = postnatal day.

Gray Matter Genotype Analysis for AQP4$^{+/+}$ and AQP4$^{-/-}$

To assess water diffusivity in GM between AQP4$^{+/+}$ and AQP4$^{-/-}$, we used DTI and T2 scans for analysis. Similar to WM results, the axial diffusivity was significantly increased in AQP4$^{-/-}$ mice at P15 ($p<0.001$, Figure 6A). In contrast to WM, the axial diffusivity in AQP4$^{-/-}$ mice were significantly lower than AQP4$^{+/+}$ at P73 and P94 ($p<0.05$). Our results indicate that enlarged ECS play a major role in resulting higher water diffusivity in AQP4$^{-/-}$ as juveniles, but the role diminishes as AQP4 channels proliferate in AQP4$^{+/+}$ mice aiding accelerated water mobility with development.

Significantly higher radial diffusivity was observed in AQP4$^{-/-}$ mice at P15, which may confirm enlarged ECS ($p<0.001$, Figure 6B). However, these findings were reversed with development. The radial diffusivity in AQP4$^{-/-}$ were significantly lower compared to AQP4$^{+/+}$ at P73 and P94 indicating the contribution of AQP4 in water mobility in maturing mice ($p<0.05$).

Next, trace diffusivity analysis revealed a significant increase in AQP4$^{-/-}$ mice at P15 confirming faster water mobility driven by enlarged ECS ($p<0.001$, Figure 6C). With development, AQP4$^{-/-}$ mice presented significantly lower trace diffusivity at P73 and P94 ($p<0.05$). Our suggestion is that AQP4 is the major component in brain water diffusivity in adulthood.

Only P15 AQP4$^{+/+}$ was found to be significantly higher than AQP4$^{-/-}$ mice in RA measurements ($p<0.001$, Figure 6D). Since RA value is inversely related to axial diffusivity, higher axial diffusivity in P15 AQP4$^{+/+}$ compared to AQP4$^{+/+}$ radial

diffusivity explains greater RA value than AQP4$^{-/-}$, where axial diffusivity is lower than radial diffusivity.

Similar to that of WM T2 results, GM T2 analysis also had notable results compared to DTI. At P15, 31% decrease in T2 values in AQP4$^{-/-}$ compared to AQP4$^{+/+}$ were observed ($p<0.001$, Figure 6E). The significance was lost at P73, but returned at P93 where a significant decrease in AQP4$^{-/-}$ was seen ($p<0.05$).

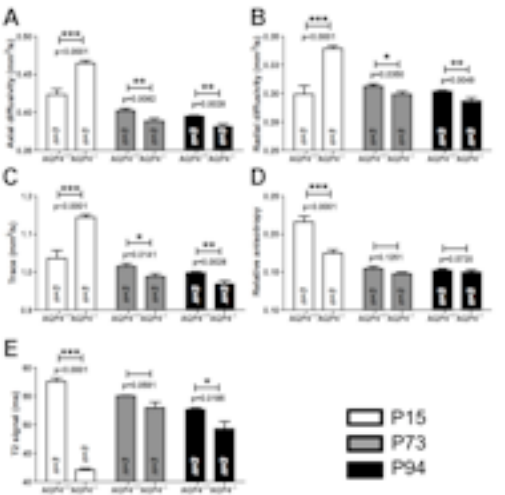

Figure 6. DTI and T2 analysis of gray matter in AQP4$^{+/+}$ and AQP4$^{-/-}$ animals. (A) The axial diffusivity was significantly increased in AQP4$^{-/-}$ mice at P15 compared to AQP4$^{+/+}$. However, at P73 and P94, AQP4$^{+/+}$ demonstrated a higher diffusivity compared to AQP4$^{-/-}$. (B) Although the radial diffusivity was significantly increased in AQP4$^{-/-}$ at P15, P73 and P94 analysis revealed significantly decreased diffusivity in AQP4$^{-/-}$. (C) P15 trace diffusivity analysis presented a significant increase in AQP4$^{-/-}$ at P15 followed by significant decrease in P73 and P94 of AQP4$^{-/-}$ mice. (D) A significantly higher RA was seen at P15. However, the significance was not seen with development. (E) T2 signal of AQP4$^{+/+}$ was significantly higher in P15 and P94. Statistical analysis was performed using unpaired *t*-tests (*p<0.05, **p<0.01, ***p<0.001). Abbreviations: P = postnatal day.

Developmental Analysis in AQP4$^{+/+}$ and AQP4$^{-/-}$

White Matter Analysis during Development in AQP4$^{+/+}$ and AQP4$^{-/-}$

To investigate developmental changes in WM diffusivities in AQP4$^{+/+}$ and AQP4$^{-/-}$, one-way and two-way ANOVA analysis were performed. Analysis of AQP4$^{+/+}$ and AQP4$^{-/-}$ during brain maturation confirmed a change of diffusivities in WM with respect to time. AQP4$^{+/+}$ mice showed a significant increase in the axial diffusivity with development ($p<0.01$, Figure 7A). In contrast, the axial diffusivity in AQP4$^{-/-}$ significantly decreased with brain maturation ($p<0.001$). These data confirm the development of glial AQP4 facilitates water mobility in AQP4$^{+/+}$ with brain maturation, and the absence of AQP4 hinders water diffusion in AQP4$^{-/-}$ in accordance with decreasing ECS size with brain development. Post-hoc Bonferroni tests confirmed significant differences between P15 and P73 ($p<0.001$) and P15 and P94 ($p<0.01$).

The radial diffusivity in both AQP4$^{+/+}$ and AQP4$^{-/-}$ significantly decreased with development ($p<0.001$, Figure 7B). These results are indicative of normal myelination in both genotypes, and the decrease in radial diffusivity with maturation supports our suggestion. Although the radial diffusivity generally decreased in both AQP4$^{+/+}$ and AQP4$^{-/-}$ with age, AQP4$^{+/+}$ presented an increased radial diffusivity from P73 to P94. We confirm that the development of AQP4 channels in AQP4$^{+/+}$ astrocytes that surround myelin allows higher water mobility perpendicular to the direction of an axon. Significant differences between

P15 and P73 ($p<0.001$) and P15 and P94 ($p<0.001$) was found using Bonferroni post-hoc tests.

Developmental analysis of trace diffusivity revealed a significant decrease in both genotypes with respect to time ($p<0.001$, Figure 7C). Interestingly, the trend of changes in trace diffusivity in both genotypes was identical to that of radial diffusivity. Our data confirm that the development of brain structures decreases water mobility with maturation. Post-hoc Bonferroni tests revealed statistically significant differences between P15 and P73 ($p<0.001$) and P15 and P94 ($p<0.001$).

RA analysis revealed significant increases in both $AQP4^{+/+}$ and $AQP4^{-/-}$ animals with brain development ($p<0.001$, Figure 7D). The increase in RA can be traced back to the formation of brain structures resulting in hindrance of water diffusivity with age.

The T2 data presented different developmental changes between the genotypes ($p<0.001$, Figure 7E). In $AQP4^{+/+}$ animals, a trend of steady decrease with maturation was observed. However, an increase from P15 to P73 followed by a decrease at P94 was seen in $AQP4^{-/-}$ subjects. Post-hoc Bonferroni tests found statistically significant differences between P15 and P73 ($p<0.001$), P15 and P94 ($p<0.001$) and P73 and P94 ($p<0.01$).

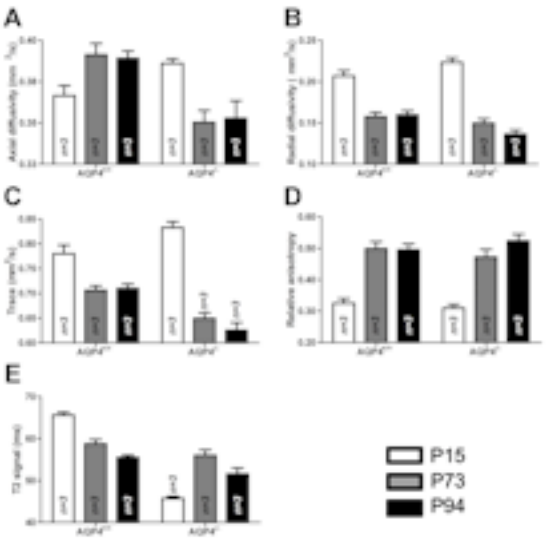

Figure 7. DTI and T2 analysis of white matter in AQP4$^{+/+}$ and AQP4$^{-/-}$ animals during development. (A) The axial diffusivity in AQP4$^{+/+}$ presented significant increase with brain maturation ($p<0.05$), whereas AQP4$^{-/-}$ showed significant decrease with maturation ($p<0.001$). (B) Both AQP4$^{+/+}$ and AQP4$^{-/-}$ showed significant decrease in the radial diffusivity with development. (C) Identical to that of radial diffusivity, trace diffusivity analysis resulted in significant decrease with respect to time in both AQP4$^{+/+}$ and AQP4$^{-/-}$. (D) Significant increase in RA with development was seen in both AQP4$^{+/+}$ and AQP4$^{-/-}$. (E) T2 signal of AQP4$^{+/+}$ showed statistically significant decrease with development. In contrast, AQP4$^{-/-}$ initially increased significantly from P15 to P77, followed by decrease at P94. Statistically significant differences between developmental groups were found in (A), (B), (C), (D) and (E) ($p<0.05$). Statistical analysis was performed using one-way ANOVA for developmental comparison within genotypes and two-way ANOVA with Bonferroni post-hoc analysis to assess interaction between genotypes with time. Abbreviations: P = postnatal day.

Gray Matter Analysis during Development in AQP4+/+ and AQP4$^{-/-}$

GM analysis was also performed to assess changes in diffusivities with brain maturation. As discussed above, one-way and two-way ANOVA analyses were used for data analysis on genotypic differences and developmental effect with time, respectively. Analysis of AQP4$^{+/+}$ and AQP4$^{-/-}$ in GM also indicated developmental changes in diffusivities. Marked decreases in the $\lambda_{\parallel}$ was found in both AQP4$^{+/+}$ and AQP4$^{-/-}$ with development ($p<0.001$; Figure 8A). Our data confirm that structural development in the brain with development resulted in decreased water mobility. Post-hoc Bonferroni tests confirmed significant differences between P15 and P73 ($p<0.001$) and P15 and P94 ($p<0.001$).

The radial diffusivity demonstrated different developmental changes between the genotypes (Figure 8B). In AQP4$^{+/+}$ subjects, an increase from P15 to P73 was seen followed by a slight decrease at P94. However, the analysis did not find statistical significance. On the contrary, AQP4$^{-/-}$ mice showed a statistically significant decrease with age ($p<0.001$). We confirm that the development of brain structures with the absence of glial AQP4 channels in AQP4$^{-/-}$ animals cause a significant decrease in water diffusion. Significant differences were found between P15 and P73 ($p<0.001$) and P15 and P94 ($p<0.001$) using post-hoc Bonferroni tests.

Trace diffusivity analysis revealed decreases in average water mobility with respect to time in both genotypes (Figure 8C). Statistically significant decreases in trace diffusivity was observed in AQP4$^{-/-}$ mice ($p<0.001$). Although

trace diffusivity of $AQP4^{+/+}$ animals steadily decreased with maturation, there was no statistical significance. $AQP4^{-/-}$ analysis confirm a general decrease of water diffusion with age due to the brain maturation as well as the absence of AQP4 channels, which facilitates water movement. Post-hoc tests revealed significant differences between P15 and P73 ($p<0.001$) and P15 and P94 ($p<0.001$) groups.

RA analysis found significant decreases in both $AQP4^{+/+}$ and $AQP4^{-/-}$ animals with brain maturation ($p<0.001$, Figure 8D). We confirm development and maturation of brain structures result in increased isotropy which reflects stabilization of structural formation. Bonferroni post-hoc tests confirmed significant differences between P15 and P73 ($p<0.001$) and P15 and P94 ($p<0.001$).

The GM T2 data demonstrated an identical trend to that of WM analysis (Figure 8E). A significant decrease with development was observed in $AQP4^{+/+}$ animals, whereas a statistically significant increase T2 signal from P15 to P73 was seen in $AQP4^{-/-}$ mice followed by decrease at P94 ($p<0.001$). Statistically significant differences were found between P15 and P73 ($p<0.001$), P15 and P94 ($p<0.001$) and P73 and P94 ($p<0.01$) using Bonferroni post-hoc tests.

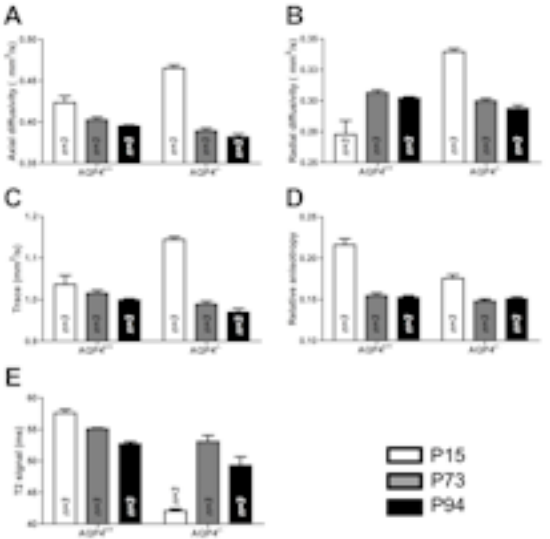

Figure 8. DTI and T2 analysis of gray matter in AQP4$^{+/+}$ and AQP4$^{-/-}$ animals during development. (A) The axial diffusivity ($\lambda_{\parallel}$) in both AQP4$^{+/+}$ and AQP4$^{-/-}$ presented significant decrease with brain development. (B) The radial diffusivity ($\lambda_{\perp}$) in AQP4$^{-/-}$ showed significant decrease with age. AQP4$^{+/+}$ analysis showed an increase from P15 to P77 and decrease at P94 with no statistical significance. (C) A significant reduction of trace diffusivity was seen only in AQP4$^{-/-}$ mice. (D) Both AQP4$^{+/+}$ and AQP4$^{-/-}$ presented significant decrease in RA with brain maturation. (E) T2 signal of AQP4$^{+/+}$ showed statistically significant reduction with development. AQP4$^{-/-}$ initially increased significantly from P15 to P77 and decreased at P94. Statistically significant differences between developmental groups were found in (A), (B), (C), (D) and (E) ($p<0.001$). Statistical analysis was performed using one-way ANOVA for developmental comparison within genotypes and two-way ANOVA with Bonferroni post-hoc analysis to assess interaction between genotypes with time. Abbreviations: P = postnatal day.

Histological Analysis

To further investigate the structural and cellular characteristics of $AQP4^{+/+}$ and $AQP4^{-/-}$ brains, IHC staining of MBP for myelination analysis and NF-200 for axonal integrity determination were performed. Consistent with previous findings of indistinguishable brain structures and myelination between $AQP4^{+/+}$ and $AQP4^{-/-}$ mice, IHC results confirmed no detectable differences in WM and GM morphology comparison (Figure 9A and B). Age matched genotype visual examination also confirmed equivalent staining intensity, cell density and distribution of MBP and NF-200 throughout all P15, P73 and P94 (not shown) in regions of WM and GM (Figure 9A and B). Our results confirm the deletion of glial AQP4 channels does not alter brain morphology.

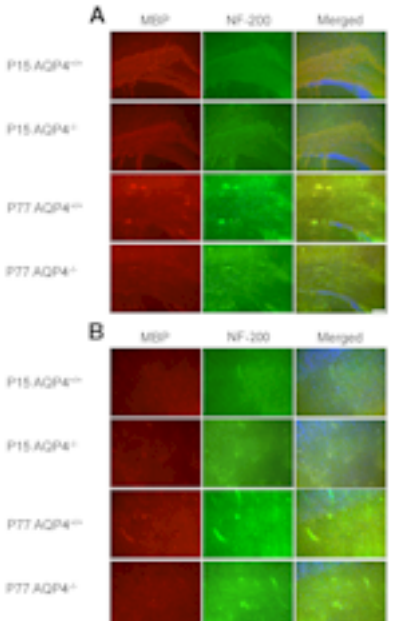

Figure 9. Immunohistochemical staining of AQP4$^{+/+}$ and AQP4$^{-/-}$ white matter (WM) and gray matter (GM) myelin basic protein (MBP) and neurofilament 200 (NF-200). (A) Assessing MBP (red), NF-200 (green), and merged images in corpus callosum (WM) were found indistinguishable at both P15 and P73 of AQP4$^{+/+}$ and AQP4$^{-/-}$. Anatomical comparison did not reveal any distinct morphological differences nor staining intensity. (B) MBP, NF-200 and merged images comparison in cortex (GM) also did not indicate notable morphological or staining intensity differences at both P15 and P73 of AQP4$^{+/+}$ and AQP4$^{-/-}$. Cellular structure and density are equivalent in all comparisons. Scale bar = 50 µm. P94 comparison (not shown) also did not reveal any differences. Abbreviations: P = postnatal day.

Brain Water Content Analysis

Having confirmed that AQP4$^{-/-}$ have enlarged ECS compared to AQP4$^{+/+}$, we last examined whether deletion of AQP4 increases basal brain water content using wet/dry mass method. Significant differences between AQP4$^{+/+}$ and AQP4$^{-/-}$ were found (Figure 10A-C). As shown in Figure 10A and C, P16 AQP4$^{-/-}$ animals exhibited lower basal water content compared to AQP4$^{+/+}$ without statistical significance. However, significantly increased brain water content was observed at P82 and P105 AQP4$^{-/-}$ ($p<0.01$). Developmental analysis of basal brain water content in AQP4$^{+/+}$ decreased significantly with maturation (one-way ANOVA, $p<0.01$; Figure 10B). In contrast, AQP4$^{-/-}$ group also displayed dramatic reduction from P16 to P82, but did not reveal significance. Taken together, our data confirm that increased brain water content in AQP4$^{-/-}$ reflects excess water in ECS. Also, basal brain water content decreases with brain maturation in AQP4$^{+/+}$ due to decrease in ECS as well as development of brain structures.

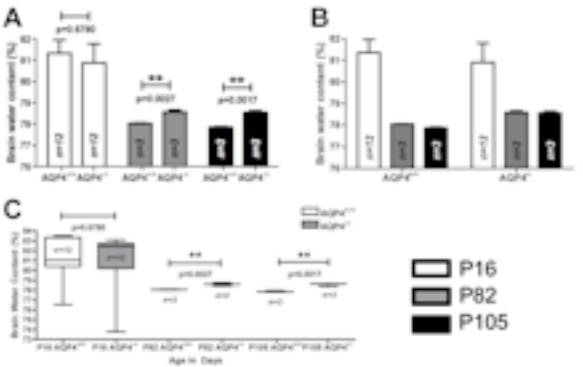

Figure 10. Baseline brain water content analysis of AQP4$^{+/+}$ and AQP4$^{-/-}$ mice. (A) Although basal brain water content comparison was not significant at P16, AQP4$^{-/-}$ at P82 and P105 were significantly higher to that of AQP4$^{+/+}$. (B) A significant decrease in brain water content with development was observed in AQP4$^{+/+}$ ($p<0.05$). AQP4$^{-/-}$ mice also presented decrease in brain water content, but was not found statistically significant. Interaction between genotypes was also not found significant. (C) Box and whisker plot representation of (A). At P16, AQP4$^{+/+}$ and AQP4$^{-/-}$ genotype did not differ significantly between genotypes. However, significantly increased brain water content in AQP4$^{-/-}$ were found at P82 and P105. The box represents the 25th-75th percentile, horizontal bars inside of boxes indicate the medians, and whiskers represent the range. Statistical analysis was performed using unpaired *t*-tests for genotype comparison, one-way ANOVA for developmental comparison within genotypes, and two-way ANOVA with Bonferroni post-hoc analysis to assess interaction between genotypes (*$p<0.05$, **$p<0.01$, ***$p<0.001$). Abbreviations: P = postnatal day.

Discussion:

This study is the first that specifically looked at water mobility in global AQP4$^{-/-}$ mice. The main purpose of this study was to compare the baseline water diffusivity difference between AQP4$^{-/-}$ and AQP4$^{+/+}$. Our investigation supports our overarching hypothesis of enlarged ECS and the absence of astrocytic AQP4 channels in AQP4$^{-/-}$ increasing water diffusivity in juveniles in comparison to AQP4$^{+/+}$, which is reversed with maturation due to the absence of AQP4 channel as well as developmental alteration of diffusivity. From this study, a significant contribution of astrocytic AQP4 channels to water diffusion is inferred. We found that global AQP4 deletion does not alter cell densities, MBP and NF-200 expression or myelination.

Effect of AQP4 Gene Deletion on Axial Diffusivity

From the DTI results it is confirmed that there are genotypic differences between AQP4$^{+/+}$ and AQP4$^{-/-}$ animals in normal conditions. The axial diffusivity was found statistically different between AQP4$^{+/+}$ and AQP4$^{-/-}$ subjects in all developmental stages in WM and GM. We observed a significantly higher axial diffusivity in P15 AQP4$^{-/-}$ mice in comparison to AQP4$^{+/+}$ animals. This significant difference in P15 mice can be traced back to the incomplete formation of brain structures, including astrocytes and oligodendrocytes. In WM, mouse brain is unmyelinated at birth and myelination does not appear until P9 and continues to P50 (Folch-Pi, 1955). AQP4 expression level at P14 was found to be 25% to that of adult levels in the cerebellum, which are similar to the cortical regions studied

for this study (Wen *et al*. 1999). Also, enlarged ECS in juvenile AQP4$^{-/-}$ provides water to diffuse more freely. Taken together, enlarged ECS in AQP4$^{-/-}$, ongoing myelination and low level of AQP4 expression in juveniles results in higher WM and GM axial diffusivity in AQP4$^{-/-}$ mice.

Significantly higher WM and GM axial diffusivity in P77 and P94 AQP4$^{+/+}$ mice was found. As discussed previously, AQP4$^{-/-}$ mice do not display any abnormal astrocytic and myelin characteristics compared to AQP4$^{+/+}$ (Saadoun *et al*. 2009). Therefore, we confirm matured astrocytes and the presence of AQP4 in AQP4$^{+/+}$ animals induce increased axial diffusivity due to accelerated water facilitation. Constrained water mobility in adult AQP4$^{-/-}$ can be traced back to the absence of AQP4, the major water channel. Although AQP4$^{-/-}$ mice have greater ECS volume fraction in adults, tissue volume fraction decreases from ~0.4 to ~0.2 by adulthood in accordance with glial proliferation, which diminishes the role of enlarged ECS in water diffusivity (Lehmenkuhler *et al*. 1993; Wen *et al*. 1999; Yao *et al*. 2008). Due to these different mechanisms at developmental stages, comparison within genotypes with respect to age showed significantly decreasing diffusivities in both WM and GM.

Effect of AQP4 Gene Deletion on Radial Diffusivity

WM genotype radial diffusivity comparisons were not found significantly different in all age groups except for P94, whereas GM comparisons were found statistically significant throughout all developmental stages. The lack of difference in WM radial diffusivity of P15 is most likely derived from the low levels of

myelination in both genotypes, and low number of AQP4 channels in $AQP4^{+/+}$ resulting in virtually equal conditions between the genotypes. Myelin begins to form from P9, but the rate of accumulation does not accelerate until P21 (Morell *et al*. 1972). As discussed previously, the level of AQP4 is about a quarter to that of adults at P14, suggesting its role is not substantial at P15 in radial water diffusion (Wen *et al*. 1999). Taken together, we suggest the basal amount of AQP4 $AQP4^{+/+}$ in P15 result in not observing significance in radial diffusivity genotype comparison. P15 GM radial diffusivity comparison presented significantly higher $AQP4^{-/-}$ diffusivity. Identical to that of axial diffusivity result, we propose low expression of AQP4 in both genotypes and enlarged ECS in $AQP4^{-/-}$ result in higher radial diffusivity in $AQP4^{-/-}$.

WM radial diffusivity analysis of P73 did not reveal significant difference. This result is consistent with a previous study where WM was stained with Luxol Fast Blue dye, which did not show difference in thickness nor staining intensity of WM in AQP4 deleted mice compared to $AQP4^{+/+}$ animals (Saadoun *et al*. 2009). In contrast to P73 WM result, P94 $AQP4^{-/-}$ radial diffusivity was found significantly lower. A decrease in number of neurons and a relative proliferation of astrocytes have been reported in aging brains (Henderson *et al*. 1980; Hayakawa *et al*. 2007). As an effect of increasing number of astrocytes in aging brains, up-regulation of AQP4s has also been observed to maintain K^+ and water homeostasis that gets disrupted with aging (Gupta and Kanungo 2011). These findings indicate that the augmentation of astrocytes and AQP4 channels in P94

AQP4$^{+/+}$ facilitate water to diffuse bidirectionally of myelin sheath and results in significantly higher radial diffusivity. In GM, both P73 and P94 AQP4$^{+/+}$ presented significantly higher radial diffusivity. We propose increased number of astrocytes and AQP4 in AQP4$^{+/+}$ facilitates increased water mobility, and the absence of AQP4 in GM and glia limitans result in decreased diffusivity in AQP4$^{-/-}$ with development.

Effect of AQP4 Gene Deletion on Trace Diffusivity and RA

Trace diffusivity and RA are derived from axial and radial diffusivities, and therefore P15 AQP4$^{-/-}$ trace diffusivity in WM and GM reflect both diffusivities. We confirmed enlarged ECS and lack of AQP4 channels in P15 as discussed above also apply to assessing trace diffusivity. In P73 and P94 mice, decreased WM and GM trace diffusivities were seen in AQP4$^{+/+}$ subjects. The mouse brain development is a reflection of the accumulation of proteins, lipids, myelin and total solids (Folch-Pi, 1955). A decrease in tissue volume fraction also occurs with this process (Lehmenkuhler *et al.* 1993; Wen *et al.* 1999). As discussed previously, inhibition of AQP4 using siRNA *in vivo* has induced decreases in ADC, an average of trace diffusivity (Badaut *et al.* 2011). Therefore, our trace diffusivity results imply that higher diffusivity in AQP4$^{-/-}$ group at P15 is ECS related, and lower diffusivities later at P73 and P94 reflect decreases in water movement due to the absence of AQP4 channels. Trace diffusivity analysis also revealed an inverse relationship of diffusivities with development. A study that

traced degrees of correlation between developing human infant brain and ADC revealed identical results which support our findings (Provenzale *et al.* 2010).

Genotype comparisons of WM and GM RA were not found significant throughout all developmental stages except for P15 GM comparison. We confirm the significantly higher RA in AQP4$^{+/+}$ P15 is most likely derived from increased ratio between axial diffusivity and radial diffusivity rather than notable morphological differences. In cases of axonal injury and TBI, a change in RA occurs due to change in brain conditions from normal state (Mac Donald *et al*. 2007). Our results imply that there is no difference in brain structure or myelination between genotypes that would cause significant difference in RA. Taken together, trace diffusivity and RA analysis confirm there are no preferential diffusivity direction in AQP4$^{-/-}$ compared to AQP4$^{+/+}$.

Histological Comparisons

Previous studies have compared BBB permeability and astrocytic expression in AQP4$^{-/-}$ subjects (Saadoun *et al.* 2009). However, no studies have examined axonal integrity of AQP4$^{-/-}$ mice. With current findings, our study looked at NF-200 and MBP characteristics to compare axonal and myelin integrity between genotypes. IHC analysis confirmed no detectable differences between genotypes. A previous study stained the corpus callosum with Luxol Fast Blue dye did not show difference in thickness of WM nor did staining intensity in AQP4 delete mice (Saadoun *et al.* 2009). Also, hippocampal NeuN staining was found to be indistinguishable between genotypes (Hsu *et al*. 2011). Manley *et al*

reported that structural MRI and light microscopy did not discover any differences in $AQP4^{+/+}$ and $AQP4^{-/-}$ mice under normal physiological states (Manley *et al.* 2004). Our findings are consistent to previously published studies that analyzed anatomical or physiological characteristics.

AQP4 Gene Deletion on Brain Baseline Water Content

Given that $AQP4^{-/-}$ mice have greater ECS, the next question was whether they contain more brain water throughout developmental stages (Yao *et al.* 2008). P82 and P105 $AQP4^{-/-}$ mice were found to have significantly higher water content. We confirm the developmental shrinkage of ECS causes a decrease in water content with age in both genotypes, and greater ECS volume fraction in $AQP4^{-/-}$ cause higher water content than $AQP4^{+/+}$. These findings are consistent with previous studies that revealed significant decrease in brain water content with development (Agrawal *et al.* 1968).

Haj-Yasein and colleagues also found significantly higher basal brain water content in both global $AQP4^{-/-}$ and conditional $AQP4^{-/-}$ mice, confirming the relationship between basal ECS volume and water content (Haj-Yasein *et al.* 2011). ECS is known to have the highest volume fraction at P0 and decreases with development (Lehmenkuhler *et al.* 1993). An interesting thing to note is that the appearance of AQP4 occurs from the second postnatal week, when there is a sudden decrease in ECS volume fraction (Lehmenkuhler *et al.* 1993; Wen *et al.* 1999). The excess brain water content in $AQP4^{-/-}$ mice is believed to reflect water content of brain parenchyma (Haj-Yasein *et al.* 2011).

Inconsistency between T2 Signal and Baseline Brain Water Content

To assess water content difference, we used T2 imaging and wet/dry mass methods. T2 values of WM and GM were found significantly lower in $AQP4^{-/-}$ of all ages. However, significantly higher water content in P82 and P105 in $AQP4^{-/-}$ was inferred from brain water content analysis. Numerous studies have linked T2 signal with water content (Knight *et al.* 1991). However, other studies have suggested signals from proteins and other molecules are also responsible for changes in T2 signal (Ochi *et al.* 1998; Qiao *et al.* 2001).

The involvement of AQP4 channels in down-regulating connexin-43 (Cx43), a major component protein in astrocytic gap junctions which plays a role in K^+ buffering, has been suggested (Nicchia *et al.* 2005; Kong *et al.* 2008). Moreover, colocalization of inwardly rectifying K^+ channel (K_{ir} 4.1) and AQP4 in glial membranes provides a functional relationship of water diffusion between AQP4 channel and K^+ buffering (Takumi *et al.* 1998; Niermann *et al.* 2001). With discussed various factors, the relationship between T2 signal and baseline brain water content remains to be further explored.

Conclusion:

The application of DTI allowed specific analysis of water diffusion in WM and GM of AQP4$^{+/+}$ and AQP4$^{-/-}$ animals. The findings confirm that deletion of AQP4 affects ECS size, brain water content and water diffusivities. The most significant finding of this study is the developmental and genotypic changes in diffusivities. Histological analysis did not exhibit any morphological nor cell density differences between AQP4$^{+/+}$ and AQP4$^{-/-}$, which confirms that brain morphology and cell density are not responsible for altering diffusivities. These findings suggest different diffusivities seen in AQP4$^{-/-}$ from AQP4$^{+/+}$ are due to enlarged ECS and the absence of AQP4 channels. Future directions could be aimed at understanding the mechanism of AQP4$^{-/-}$ mice in terms of diffusivities and other possible contributing factors. Further understanding of different baseline diffusivities may lead to provide new insights and targets for control of brain edema and seizure.

Bibliography

Agrawal, H. C., J. M. Davis, et al. (1968). "Developmental changes in mouse brain: weight, water content and free amino acids." J Neurochem **15**(9): 917-923.

Agre, P. (2006). "The aquaporin water channels." Proc Am Thorac Soc **3**(1): 5-13.

Agre, P., L. S. King, et al. (2002). "Aquaporin water channels--from atomic structure to clinical medicine." J Physiol **542**(Pt 1): 3-16.

Alexander, A. L., J. E. Lee, et al. (2007). "Diffusion tensor imaging of the brain." Neurotherapeutics **4**(3): 316-329.

Auguste, K. I., S. Jin, et al. (2007). "Greatly impaired migration of implanted aquaporin-4-deficient astroglial cells in mouse brain toward a site of injury." FASEB J **21**(1): 108-116.

Badaut, J., S. Ashwal, et al. (2011). "Brain water mobility decreases after astrocytic aquaporin-4 inhibition using RNA interference." J Cereb Blood Flow Metab **31**(3): 819-831.

Binder, D. K., K. Oshio, et al. (2004). "Increased seizure threshold in mice lacking aquaporin-4 water channels." Neuroreport **15**(2): 259-262.

Binder, D. K., M. C. Papadopoulos, et al. (2004). "In vivo measurement of brain extracellular space diffusion by cortical surface photobleaching." J Neurosci **24**(37): 8049-8056.

Binder, D. K., X. Yao, et al. (2006). "Increased seizure duration in mice lacking aquaporin-4 water channels." Acta Neurochir Suppl **96**: 389-392.

Binder, D. K., X. Yao, et al. (2006). "Increased seizure duration and slowed potassium kinetics in mice lacking aquaporin-4 water channels." Glia **53** (6): 631-636.

Bloch, O., K. I. Auguste, et al. (2006). "Accelerated progression of kaolin-induced hydrocephalus in aquaporin-4-deficient mice." J Cereb Blood Flow Metab **26**(12): 1527-1537.

Bloch, O., M. C. Papadopoulos, et al. (2005). "Aquaporin-4 gene deletion in mice increases focal edema associated with staphylococcal brain abscess." J Neurochem **95**(1): 254-262.

Buonanno, F. S., I. L. Pykett, et al. (1983). "Proton NMR imaging in experimental ischemic infarction." Stroke **14**(2): 178-184.

Folch-Pi, J. (1955). “In Biochemistry of the Developing Nervous System (Edited by Waelsch H.).” Academic Press: 121.

Gupta, R. K. and M. Kanungo (2011). "Glial molecular alterations with mouse brain development and aging: up-regulation of the Kir4.1 and aquaporin-4." Age (Dordr).

Gwan, K. and H. T. Edzes (1975). "Water in brain edema. Observations by the pulsed nuclear magnetic resonance technique." Arch Neurol **32**(7): 462-465.

Haj-Yasein, N. N., G. F. Vindedal, et al. (2011). "Glial-conditional deletion of aquaporin-4 (Aqp4) reduces blood-brain water uptake and confers barrier function on perivascular astrocyte endfeet." Proc Natl Acad Sci U S A **108** (43): 17815-17820.

Hayakawa, N., H. Kato, et al. (2007). "Age-related changes of astorocytes, oligodendrocytes and microglia in the mouse hippocampal CA1 sector." Mech Ageing Dev **128**(4): 311-316.

Henderson, G., B. E. Tomlinson, et al. (1980). "Cell counts in human cerebral cortex in normal adults throughout life using an image analysing computer." J Neurol Sci **46**(1): 113-136.

Hsu, M. S., D. J. Lee, et al. (2007). "Potential role of the glial water channel aquaporin-4 in epilepsy." Neuron Glia Biol **3**(4): 287-297.

Hsu, M. S., M. Seldin, et al. (2011). "Laminar-specific and developmental expression of aquaporin-4 in the mouse hippocampus." Neuroscience **178**: 21-32.

Knight, R. A., R. J. Ordidge, et al. (1991). "Temporal evolution of ischemic damage in rat brain measured by proton nuclear magnetic resonance imaging." Stroke **22**(6): 802-808.

Kong, H., Y. Fan, et al. (2008). "AQP4 knockout impairs proliferation, migration and neuronal differentiation of adult neural stem cells." J Cell Sci **121**(Pt 24): 4029-4036.

Lee, D. J., M. Amini, et al. (2012). "Aquaporin-4-dependent edema clearance following status epilepticus." Epilepsy Res **98**(2-3): 264-268.

Lee, T. S., T. Eid, et al. (2004). "Aquaporin-4 is increased in the sclerotic hippocampus in human temporal lobe epilepsy." Acta Neuropathol **108**(6): 493-502.

Lehmenkuhler, A., E. Sykova, et al. (1993). "Extracellular space parameters in the rat neocortex and subcortical white matter during postnatal development determined by diffusion analysis." Neuroscience **55**(2): 339-351.

Ma, T., B. Yang, et al. (1997). "Generation and phenotype of a transgenic knockout mouse lacking the mercurial-insensitive water channel aquaporin-4." J Clin Invest **100**(5): 957-962.

Mac Donald, C. L., K. Dikranian, et al. (2007). "Diffusion tensor imaging reliably detects experimental traumatic axonal injury and indicates approximate time of injury." J Neurosci **27**(44): 11869-11876.

Manley, G. T., D. K. Binder, et al. (2004). "New insights into water transport and edema in the central nervous system from phenotype analysis of aquaporin-4 null mice." Neuroscience **129**(4): 983-991.

Manley, G. T., M. Fujimura, et al. (2000). "Aquaporin-4 deletion in mice reduces brain edema after acute water intoxication and ischemic stroke." Nat Med **6**(2): 159-163.

Mori, S., R. Itoh, et al. (2001). "Diffusion tensor imaging of the developing mouse brain." Magn Reson Med **46**(1): 18-23.

Nagelhus, E. A., T. M. Mathiisen, et al. (2004). "Aquaporin-4 in the central nervous system: cellular and subcellular distribution and coexpression with KIR4.1." Neuroscience **129**(4): 905-913.

Naruse, S., Y. Horikawa, et al. (1982). "Proton nuclear magnetic resonance studies on brain edema." J Neurosurg **56**(6): 747-752.

Nicchia, G. P., A. Frigeri, et al. (2003). "Inhibition of aquaporin-4 expression in astrocytes by RNAi determines alteration in cell morphology, growth, and water transport and induces changes in ischemia-related genes." FASEB J **17**(11): 1508-1510.

Nicchia, G. P., M. Srinivas, et al. (2005). "New possible roles for aquaporin-4 in astrocytes: cell cytoskeleton and functional relationship with connexin43." FASEB J **19**(12): 1674-1676.

Nicholson, C. and J. M. Phillips (1981). “Ion diffusion modified by volume fraction and tortuosity in the extracellular microenvironment of the rat cerebellum.” J Physiol **321**: 225-257.

Nielsen, S., E. A. Nagelhus, et al. (1997). "Specialized membrane domains for water transport in glial cells: high-resolution immunogold cytochemistry of aquaporin-4 in rat brain." J Neurosci **17**(1): 171-180.

Niermann, H., M. Amiry-Moghaddam, et al. (2001). "A novel role of vasopressin in the brain: modulation of activity-dependent water flux in the neocortex." J Neurosci **21**(9): 3045-3051.

Obenaus, A. and S. Ashwal (2008). "Magnetic resonance imaging in cerebral ischemia: focus on neonates." Neuropharmacology **55**(3): 271-280.

Obenaus, A. and R. E. Jacobs (2007). "Magnetic resonance imaging of functional anatomy: use for small animal epilepsy models." Epilepsia **48 Suppl 4**: 11-17.

Ochi, M., K. Hayashi, et al. (1998). "Unusual CT and MR appearance of an epidermoid tumor of the cerebellopontine angle." AJNR Am J Neuroradiol **19**(6): 1113-1115.

Papadopoulos, M. C., G. T. Manley, et al. (2004). "Aquaporin-4 facilitates reabsorption of excess fluid in vasogenic brain edema." FASEB J **18**(11): 1291-1293.

Papadopoulos, M. C. and A. S. Verkman (2005). "Aquaporin-4 gene disruption in mice reduces brain swelling and mortality in pneumococcal meningitis." J Biol Chem **280**(14): 13906-13912.

Provenzale, J. M., J. Isaacson, et al. (2010). "Correlation of apparent diffusion coefficient and fractional anisotropy values in the developing infant brain." AJR Am J Roentgenol **195**(6): W456-462.

Qiao, M., K. L. Malisza, et al. (2001). "Correlation of cerebral hypoxic-ischemic T2 changes with tissue alterations in water content and protein extravasation." Stroke **32**(4): 958-963.

Saadoun, S., B. A. Bell, et al. (2008). "Greatly improved neurological outcome after spinal cord compression injury in AQP4-deficient mice." Brain **131**(Pt 4): 1087-1098.

Saadoun, S., M. C. Papadopoulos, et al. (2005). "Impairment of angiogenesis and cell migration by targeted aquaporin-1 gene disruption." Nature **434** (7034): 786-792.

Saadoun, S., M. C. Papadopoulos, et al. (2005). "Involvement of aquaporin-4 in astroglial cell migration and glial scar formation." J Cell Sci **118**(Pt 24): 5691-5698.

Saadoun, S., M. J. Tait, et al. (2009). "AQP4 gene deletion in mice does not alter blood-brain barrier integrity or brain morphology." Neuroscience **161**(3): 764-772.

Scholz, T. D., S. R. Fleagle, et al. (1990). "Effect of tissue fat and water content on nuclear magnetic resonance relaxation times of cardiac and skeletal muscle." Magn Reson Imaging **8**(5): 605-611.

Solenov, E., H. Watanabe, et al. (2004). "Sevenfold-reduced osmotic water permeability in primary astrocyte cultures from AQP-4-deficient mice, measured by a fluorescence quenching method." Am J Physiol Cell Physiol **286**(2): C426-432.

Solenov, E. I., L. Vetrivel, et al. (2002). "Optical measurement of swelling and water transport in spinal cord slices from aquaporin null mice." J Neurosci Methods **113**(1): 85-90.

Sun, S. W., J. J. Neil, et al. (2003). "Relative indices of water diffusion anisotropy are equivalent in live and formalin-fixed mouse brains." Magn Reson Med **50**(4): 743-748.

Sun, S. W., S. K. Song, et al. (2003). "Directional correlation characterization and classification of white matter tracts." Magn Reson Med **49**(2): 271-275.

Tait, M. J., S. Saadoun, et al. (2008). "Water movements in the brain: role of aquaporins." Trends Neurosci **31**(1): 37-43.

Takumi, Y., E. A. Nagelhus, et al. (1998). "Select types of supporting cell in the inner ear express aquaporin-4 water channel protein." Eur J Neurosci **10** (12): 3584-3595.

Thiagarajah, J. R., M. C. Papadopoulos, et al. (2005). "Noninvasive early detection of brain edema in mice by near-infrared light scattering." J Neurosci Res **80**(2): 293-299.

Unger, E., J. Littlefield, et al. (1988). "Water content and water structure in CT and MR signal changes: possible influence in detection of early stroke." AJNR Am J Neuroradiol **9**(4): 687-691.

Verkman, A. S. (2002). "Physiological importance of aquaporin water channels." Ann Med **34**(3): 192-200.

Verkman, A. S. (2005). "More than just water channels: unexpected cellular roles of aquaporins." J Cell Sci **118**(Pt 15): 3225-3232.

Verkman, A. S., D. K. Binder, et al. (2006). "Three distinct roles of aquaporin-4 in brain function revealed by knockout mice." Biochim Biophys Acta **1758**(8): 1085-1093.

Wen, H., E. A. Nagelhus, et al. (1999). "Ontogeny of water transport in rat brain: postnatal expression of the aquaporin-4 water channel." Eur J Neurosci **11** (3): 935-945.

Yao, X., S. Hrabetova, et al. (2008). "Aquaporin-4-deficient mice have increased extracellular space without tortuosity change." J Neurosci **28**(21): 5460-5464.

Zador, Z., M. Magzoub, et al. (2008). "Microfiberoptic fluorescence photobleaching reveals size-dependent macromolecule diffusion in extracellular space deep in brain." FASEB J **22**(3): 870-879.
contact with blood vessels and astrocyte membranes that ensheathe synapses